Appl Biochem Biotechnol (2010) 160:831–842
DOI 10.1007/s12010-008-8470-2

Structural Analysis and Inhibitory Kinetics of Brain Type Creatine Kinase by Sodium Dodecyl Sulfate

Zhi-Rong Lü · Sang Ho Oh · Shan-Shan Zhou · He-Chang Zou · Daeui Park · Seong Jin Park · Hong-Wei Zhou · Jong Bhak · Yong-Doo Park · Fei Zou

Received: 24 October 2008 / Accepted: 2 December 2008 /
Published online: 13 December 2008

Abstract The studies regarding the effect of sodium dodecyl sulfate (SDS) on enzyme activities and structures can provide a valuable insight into public health. We have predicted the 3D structure of the brain creatine kinase (CK-BB) with a high resolution and simulated the docking between CK-BB and SDS. The predicted structure had a root mean square deviation of 0.51 Å. The docking between CK-BB and SDS was successful with significant scores (−4.67 kcal/mol, AutoDock4 and −48.32 kcal/mol, DOCK6). We have also investigated the inactivation by using SDS to study CK-BB's folding behaviors. The two-phase rate constants as a first-order reaction were measured during inactivation. SDS strongly inhibited the CK-BB activity in a noncompetitive inhibition manner (K_i= 1.22 mM). The tertiary structural change was induced by SDS binding with the exposure of hydrophobic surface. The methyl-β-cyclodextrin was used to strip SDS from the enzyme molecule to reactivate. The changes of thermodynamic parameters for the SDS ligand binding such as enthalpy, Gibbs free energy, and entropy were obtained as −13±7.0 MJ/mol, 8.39 kJ/mol, and −42.754 kJ/(K mol), respectively. Our study provides important structural information for CK-BB and its interaction with SDS with an insight on its folding and inhibition kinetics.

Keywords Brain creatine kinase · Sodium dodecyl sulfate · Structure prediction · Folding · Thermodynamics

Z.-R. Lü · S.-S. Zhou · H.-W. Zhou · Y.-D. Park · F. Zou (✉)
Department of Environmental Health, School of Public Health and Tropical Medicine,
Southern Medical University, Baiyun District, North of Guangzhou Road No.1838, Guangzhou 510515,
People's Republic of China
e-mail: zoufei_dean@hotmail.com

S. H. Oh · D. Park · S. J. Park · J. Bhak
Korean BioInformation Center (KOBIC), KRIBB, Daejeon 305-806, South Korea

H.-C. Zou · Y.-D. Park
Yangtze Delta Region Institute of Tsinghua University, Jiaxing 314050, People's Republic of China

Abbreviations

CK-BB	Brain type creatine kinase
SDS	Sodium dodecyl sulfate
M-β-CD	Methyl-β-cyclodextrin
ANS	1-Anilinonaphthalene-8-sulfonate
RMSD	Root mean square deviation
DOPE	Discrete optimized protein energy

Introduction

Protein denaturation studies have provided insights to understand enzyme structures that are related to catalysis and stability affected by forces that are to maintain tertiary structures, conformational flexibility, compactness, and folding. The most frequently applied denaturants used for protein folding studies are sodium dodecyl sulfate (SDS), guanidine hydrochloride, and urea. These denaturants have shown different characteristics of protein folding and were used to investigate different enzyme structural characteristics. It is generally recognized that the sulfate group and alkyl chain of SDS can interact with proteins via interactions with positively charged amino acid side chains as well as hydrophobic side chains. Usually SDS-denatured proteins retain a large degree of ordered structure in contrast to either guanidine hydrochloride or urea. From the environmental aspects, SDS is abundantly present with frequent contact by people due to a high level of usage in modern life. Therefore, the studies regarding the effect of SDS on enzyme activities and structures can provide a valuable insight into public health.

Creatine kinase (CK; ATP: creatine *N*-phosphotransferase, EC 2.7.3.2) is a cytoplasmic enzyme involved in energy homeostasis. The catalytic reaction by CK is ATP + creatine ↔ ADP + phosphocreatine. It acts as a homodimer in the brain and some other tissues. It is sometimes found as a heterodimer isozyme in the heart. Muscle and brain types of CK are the most commonly found, and three different isoenzymes including CK-MM (the muscle type homodimer), CK-BB (the brain type homodimer), and CK-MB (the muscle plus brain type heterodimer) originate from these two common types. In addition, two mitochondrial types of CK, such as the ubiquitous and sarcomeric forms, are also found in tissues [1, 2]. In this regard, several physical properties of CK isozymes, both as homo- and heterodimers, were compared to understand how the hybrid modifies subunit conformation and dynamics [3]. It is well known that CK is important not only in the diagnosis of myocardial infarction (an important serum marker), cardiac hypertrophy, and muscular dystrophy, but also for the studies of other serious diseases, including Alzheimer's disease, Parkinson's disease, and psoriasis [4–9]. However, the CK-BB characteristic in respect to enzyme structure and stability by using denaturants has not been carried out yet.

Here, we conducted a 3D computational prediction of CK-BB and a real-time inactivation analysis in the presence of SDS in order to understand the structural and function mechanisms of CK-BB in association with SDS. Our computational docking suggested that SDS can bind with CK-BB tightly by the active site pocket and, hence, induce the inactivation. The kinetics showed that SDS-induced inactivation followed the first-order reaction, and this is coupled with structural changes as well as transition free energy change ($\Delta\Delta G^{\circ\prime}$) increases. Cyclodextrin could directly strip the SDS from CK-BB and reactivate the activity with a monophasic process. In addition, thermodynamic parameters by the isothermal titration microcalorimetry were measured to elucidate the ligand-binding mechanism between SDS and CK-BB.

Materials and Methods

Materials and Assay of CK-BB Activity

Recombinant human CK-BB was expressed and purified according to the previous reports [10, 11]. CK-BB purity was confirmed by one band both in SDS- and native-PAGE analyses coupled with LC–MS/MS identification. SDS and methyl-β-cyclodextrin (M-β-CD) were purchased from Sigma. CK-BB activity was measured following proton generation during the reaction of ATP and creatine with the indicator thymol blue at 597 nm at 25 °C. The substrate was composed of 24 mM creatine, 4 mM ATP, 8 mM magnesium acetate, 0.01% thymol blue, and 5 mM glycine–NaOH (pH 9.0). All the other reagents were analytical grade local products.

Homology Modeling of CK-BB Structure

The 3D model of CK-BB comprising of 381 amino acids (NCBI entry: NP_001814) was built using MODELLER9v1 [12] based on homology modeling [13]. The MODELLER program automatically provides an all-atom model using alignments between the query sequence and known homologous structures. We retrieved the known homologous structures of CK-BB from the Protein Data Bank (PDB; http://www.pdb.org). We found that bovine retinal creatine kinase chain A (PDB entry: 1g0w) was a very good structural template (97% sequence identity) as a close homologue for CK-BB. A sequence alignment between CK-BB and 1g0w was constructed by ALIGN2D in the MODELLER package. Based on the sequence alignment, the 3D structure of CK-BB was constructed with a high level of confidence. Then, we calculated the conformational energy of a structural model, CK-BB, with the discrete optimized protein energy (DOPE) score as the stability measure. We also calculated the root mean square deviation (RMSD) between the predicted structure and the template structure using the SHEBA program [14]. To evaluate the overall structural integrity, we aligned the predicted structure in the dimeric structure of the native template structures. The structural alignment or the superimposition with 1g0w was straightforward due to their high homology levels. The dimer structure of 1g0w was retrieved from PDBsum (http://www.pdbsum.org).

In Silico Docking of CK-BB Structure and SDS

There are many tools available for an in silico protein-ligand docking. AutoDock4 and DOCK6 are the most commonly used for their automated docking capability. The programs also perform the ligand docking to a set of predefined 3D grids of the target protein. However, AutoDock uses a random search technique [15], and DOCK uses a systemic search technique [16]. Therefore, we used two slightly different approaches for the dockings of CK-BB and SDS. The original structure of SDS was derived from the PubChem database (Compound ID: 34232652; http://www.pubchem.org) [17]. Several steps of the docking preparation procedure are categorized to (1) converting 2D to 3D, (2) calculating charges, (3) adding hydrogen atoms, and (4) finding pockets. For these steps, we used the fconverter program of the J-Chem package (http://www.chemaxon.com/) and OpenBabel (http://openbabel.sourceforge.org).

Intrinsic and 1-Anilinonaphthalene-8-Sulfonate-Binding Fluorescence Measurements

The fluorescence emission spectra were measured with an F-2500 Fluorescence Spectrophotometer using a 1-cm path-length cuvette. An excitation wavelength of 280 nm was used for the tryptophan fluorescence measurement, and the emission

wavelengths ranged between 300 and 410 nm. The hydrophobic fluorescence changes were studied by 50 μM 1-anilinonaphthalene-8-sulfonate (ANS) labeling for 30 min prior to measurement. An excitation wavelength of 390 nm was used for the ANS-binding fluorescence, and the emission wavelengths ranged from 400 to 600 nm.

Isothermal Titration Microcalorimetry

Isothermal titration microcalorimetric measurements were performed with a 3101 TAM III Thermostat (Thermometric AB, Järfälla, Sweden) in accordance with a previous report [18]. TAM Assistant™ software was used for operations and calculating the parameters. SDS titration to CK-BB was conducted under the following conditions: the ampoule volume was 800 μl; the ampoule concentrations were 10 μM CK-BB; the syringe concentration was 200 mM SDS; the injection volume was 10 μl; there were 20 injection times with 3 min intervals between them, and the stirring rate was 90 rpm. The "feedback" mode was used for the measurements. The equilibrium constant (K) and the change of enthalpy (ΔH) were obtained from the fitted data. Gibbs free energy change (ΔG) and the entropy change (ΔS) were calculated from the software's instructions, respectively. All the measurements were carried out at 25 °C (298 K).

Results and Discussion

Computational Prediction of CK-BB 3D Structure and SDS Docking Simulation

In homology modeling, the accuracy of structure prediction depends strongly on template structures. Considering sequence identity, DOPE score, and RMSD score, we selected a

```
 _aln.pos          10        20        30        40        50        60
1g0w_A    -PFSNSHNTLKLRFPAEDEFPDLSGHNNHMAKVLTPELYAELRAKSTPSGFTVDDVIQTGVDNPGHPY
CKB       MPFSNSHNALKLRFPAEDEFPDLSAHNNHMAKVLTPELYAELRAKSTPSGFTLDDVIQTGVDNPGHPY
 _consrvd  ******* *************** ************************* ***************

 _aln.p   70        80        90       100       110       120       130
1g0w_A    IMTVGCVAGDEESYDVFKELFDPIIEDRHGGYKPTDEHKTDLNPDNLQGGDDLDPNYVLSSRVRTGRS
CKB       IMTVGCVAGDEESYEVFKDLFDPIIEDRHGGYKPSDEHKTDLNPDNLQGGDDLDPNYVLSSRVRTGRS
 _consrvd ************** *** *************** ********************************

 _aln.pos  140       150       160       170       180       190       200
1g0w_A    IRGFCLPPHCSRGERRAIEKLAVEALSSLDGDLAGRYYALKSMTEAEQQQLIDDHFLFDKPVSPLLLA
CKB       IRGFCLPPHCSRGERRAIEKLAVEALSSLDGDLAGRYYALKSMTEAEQQQLIDDHFLFDKPVSPLLLA
 _consrvd ************************************************************************

 _aln.pos    210       220       230       240       250       260       270
1g0w_A    SGMARDWPDARGIWHNDNKTFLVWINEEDHLRVISMQKGGNMKEVFTRFCNGLTQIETLFKSKNYEFM
CKB       SGMARDWPDARGIWHNDNKTFLVWVNEEDHLRVISMQKGGNMKEVFTRFCTGLTQIETLFKSKDYEFM
 _consrvd ************************ ************************ ************ ****

 _aln.pos      280       290       300       310       320       330       340
1g0w_A    WNPHLGYILTCPSNLGTGLRAGVHIKLPHLGKHEKFSEVLKRLRLQKRGV--------GGVFDVSNAD
CKB       WNPHLGYILTCPSNLGTGLRAGVHIKLPNLGKHEKFSEVLKRLRLQKRGTGGVDTAAVGGVFDVSNAD
 _consrvd ***************************** ******************         **********

 _aln.pos        350       360       370       380
1g0w_A    RLGFSEVELVQMVVDGVKLLIEMEQRLEQGQAIDDLMPAQK
CKB       RLGFSEVELVQMVVDGVKLLIEMEQRLEQGQAIDDLMPAQK
 _consrvd ****************************************
```

Fig. 1 CK-BB and 1g0w sequence alignment result. A sequence alignment between the CK-BB and the 1g0w was constructed by ALIGN2D in the MODELLER package. 1g0w indicates a PDB entry for bovine retinal creatine kinase chain A

template structure (PDB entry: 1g0w; Fig. 1). The sequence identity was 97%, and the resulting model's RMSD score was 0.51 Å which is extremely high as a model (Fig. 2). Also, DOPE scores were almost the same (CK-BB −42,523 and 1G0W −43,656) which means the model structure was nearly a native structure (Table 1). It is known that MODELLER can predict structures with an almost 100% accuracy with structural templates that have over 90% sequence identities [12]. In our prediction, there was a highly homologous template for CK-BB. In the predicted structure of CK-BB, we found a single large binding pocket (pocket size 2,440 $Å^3$) per subunit. Often, the largest pockets in proteins function as binding pockets, and we concluded that the large pocket of CK-BB is a probable binding site. With the AutoDock and DOCK results, we searched for SDS-interacting residues of CK-BB which are close in distance, namely, under a 3.0-Å distance (DOCK: ARG132, SER309, LYS313, ARG320, and ARG341; AutoDock: ARG132, ARG290, ARG320, and ARG341). We accepted the residues that are commonly interacting with SDS as the most important binding residues between CK-BB and SDS. They are ARG132, ARG320, and ARG341 (Fig. 3).

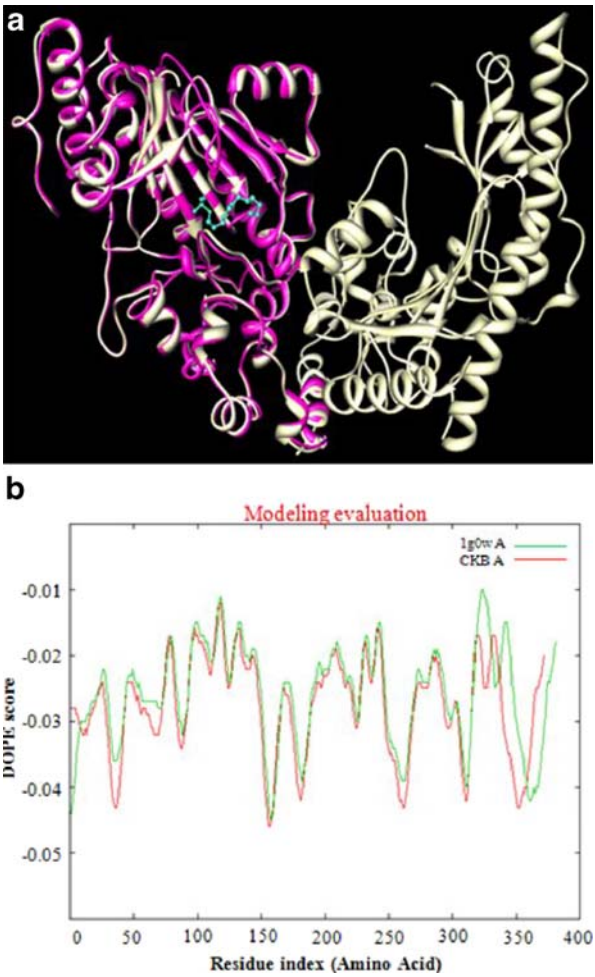

Fig. 2 CK-BB prediction structure superimposed 1g0w chain A. **a** 3D CK-BB prediction structure with a SDS molecule. A structural alignment of the CK-BB and the 1g0w was constructed by SHEBA. In the figure, the *white ribbon* is 1g0w chain A and B of dimeric structure from PDBsum. The *pink ribbon* is CK-BB chain A, and *spring green stick* is SDS. **b** DOPE score. A DOPE score by residues of the CK-BB and the 1g0w was constructed by assessing DOPE in the MODELLER package

Table 1 The accuracy of predicted CK-BB structures.

CK-BB chain	DOPE score	1g0w	
		RMSD (Å)	DOPE
Chain A	−42,523.6250	0.51	−43,418.6719
Chain B	−43,656.6680	1.76	−43,418.4023

The Effect of SDS on the Activity of CK-BB and Kinetics

The recombinant human CK-BB was inactivated with various concentrations of SDS. An equilibrium state of the inactivated CK-BB with no further activity change was reached after 2 h incubation with SDS (Fig. 4a). Although almost all the activity was eliminated by SDS, CK-BB was never completely inactivated (4% to 5% activity was still sustained), regardless of increased incubation time or SDS concentration. This is probably caused by the stable denatured complex between the enzyme and SDS in the SDS micelles. The Lineweaver–Burk plot for SDS inhibition is given in Fig. 4b. The results indicate that SDS is a noncompetitive inhibitor at the creatine-binding site. K_i value was obtained from the secondary replot of apparent V_{max} versus [SDS] and calculated as 1.22 mM. To detect inactivation kinetics and rate constants, time-interval measurements were performed (Fig. 4c). The results showed that the enzyme activity gradually decreased in a time-dependent manner in the presence of various concentrations of SDS.

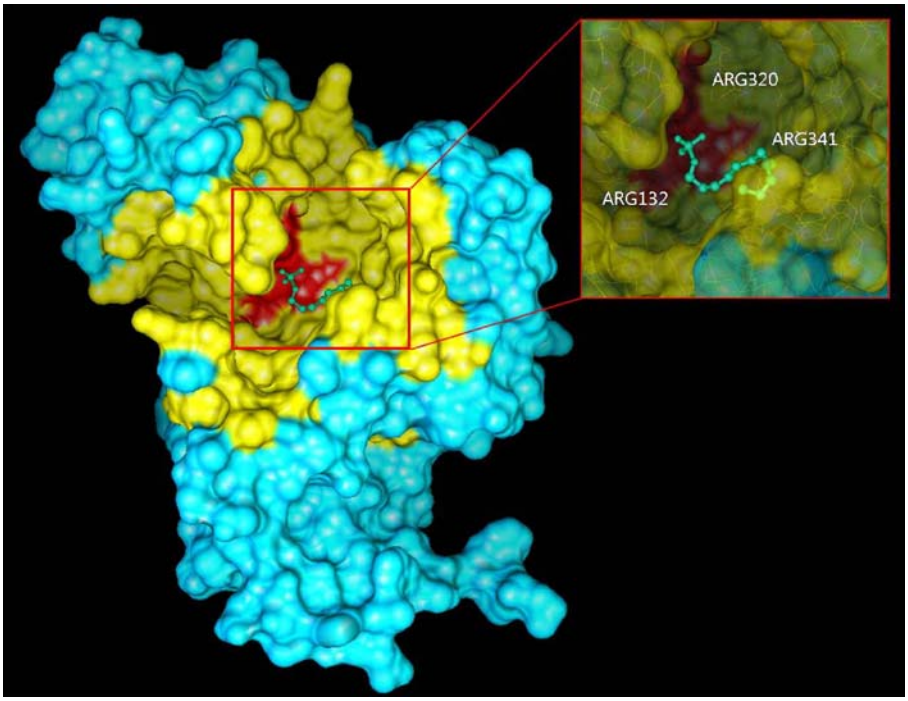

Fig. 3 Computational docking result for CK-BB and SDS. The *yellow region* in CK-BB is the biggest pocket site (pocket size 2,440 Å^3), and the *green stick* is SDS. *Right box* indicates SDS-binding site with residue of ARG132, ARG320, and ARG341

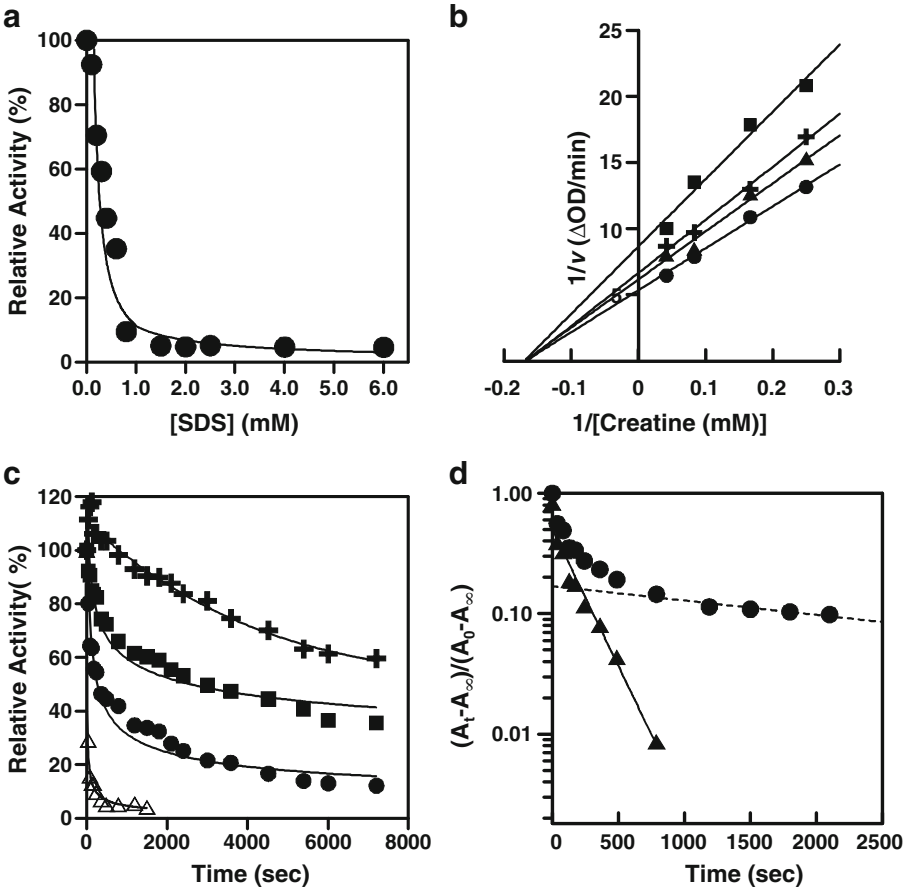

Fig. 4 Effect of SDS on the activity of CK-BB. a Inactivation of CK-BB by different concentrations of SDS. The remaining activity was measured after the enzyme was mixed with the reaction mixture for 2 h. **B** Lineweaver–Burk plots. SDS concentrations were: 0 (*filled circle*), 0.3 (*filled triangle*), 0.4 (*plus sign*), and 0.8 mM (*filled square*). **c** Inactivation kinetics. The enzyme solutions were mixed with various concentrations of SDS: 0.2 mM (*plus sign*), 0.4 mM (*filled square*), 0.75 mM (*filled circle*), and 1.0 mM (*empty triangle*), and aliquots were taken at the indicated time intervals. **d** The semilogarithmic plot in the presence of 0.85 mM SDS. *Filled circle*, experimental points. *Filled triangle*, points obtained by subtracting the contribution of the slow phase from the data in the curve (*dashed line*). Slopes of the curves (*solid line* or *dashed line*) indicate the rate constants. The final enzyme concentrations were 2.0 μM in the reaction mixture and 0.02 μM in the assay system

Subsequent kinetic studies from the semilogarithmic plot analysis showed the biphasic inactivation, fast (k_1) and slow (k_2; Fig. 4d). Microscopic inactivation rate constants are summarized in Table 2: the inactivation occurred with the changes of transition free energy ($\Delta\Delta G^{\circ\prime}$), which were decreased with a SDS concentration-dependent manner. The phenomenon of the biphasic inactivation process implied that CK-BB passed transiently existed intermediates until it reached a completely unfolded state. It was probably caused by the accumulation of intermediates as with the increasing denaturants concentration. The disruption of the active site conformation by denaturant occurred very quickly

Table 2 Microscopic inactivation rate constants of CK-BB in the presence of SDS.

SDS (mM)	Inactivation rate constants ($\times 10^{-3}$ s^{-1})[a]		Transition free energy change (kJ/mol min^{-1})[b]
	k_1	k_2	
0.2	0.31	–	30.16
0.4	4.55	0.3	23.50
0.75	9.23	0.45	21.75
1.0	27.2	1.7	19.07

[a] Data were calculated as shown in Fig. 2b. k_1 and k_2 are the first-order rate constants for the fast and slow phases, respectively

[b] According to Tams and Welinder [19] with slight modification, transition free energy change per minute, $\Delta\Delta G^{\circ\prime}=-RT\ln k'$, where k' is a time constant for the major phase of the inactivation reaction

accompanied by the loss of the highest activity, then it underwent a slow phase, and partially unfolded states of transient intermediates underwent a slow inactivation until it became completely unfolded.

The Effect of SDS on the Tertiary Structure of CK-BB

The tertiary structural changes of CK-BB in the presence of SDS were measured (Fig. 5). From the results of the intrinsic fluorescence spectra, we observed that SDS binding to the CK-BB resulted in conformational changes: the spectra gradually decreased without a significant wavelength peak shift in a dose-dependent manner (Fig. 5a). In accordance, the hydrophobic surface was exposed by SDS detected with ANS dye binding. A more than 50% increase of hydrophobicity compared to the native control was observed even under the low concentration of SDS (Fig. 5b). From the docking simulation and above results, we concluded that the structural change by SDS binding occurred regionally, mostly at the active site. Therefore, the hydrophobic surface exposure was significant compared to the overall structural change.

Application of the SDS–Cyclodextrin Mechanism as an Artificial Chaperone to Reactivate CK-BB

When M-β-CD described as an artificial chaperone [20] was added into the incubation solution that contained the fixed concentration of SDS (6 mM) with CK-BB, the enzyme activity was recovered in M-β-CD dose-dependent manner (Fig. 6a). The degrees of reactivity were almost 60% recovered to the native state within 1 h. The reactivation process had a monophase kinetic course after treatment with M-β-CD (Fig. 6b, c), which was different from the biphasic kinetic courses of inactivation. The relationship between apparent reactivation constants and M-β-CD is described in Fig. 6d, showing that enhancement of M-β-CD concentration accelerated the rate of reactivation.

Critical micelle concentration of SDS is empirically known to unfold polypeptide chains and induce complete inactivation. CK-BB was found to have relatively sensitive responses toward SDS, though denaturation never reached the complete inactivation in the concentration of SDS micelle, and inactivation of the residual activity needs a long time when SDS concentration is low. From the aspect of protein unfolding, CK-BB structure change is closely coupled with active site conformational changes which was

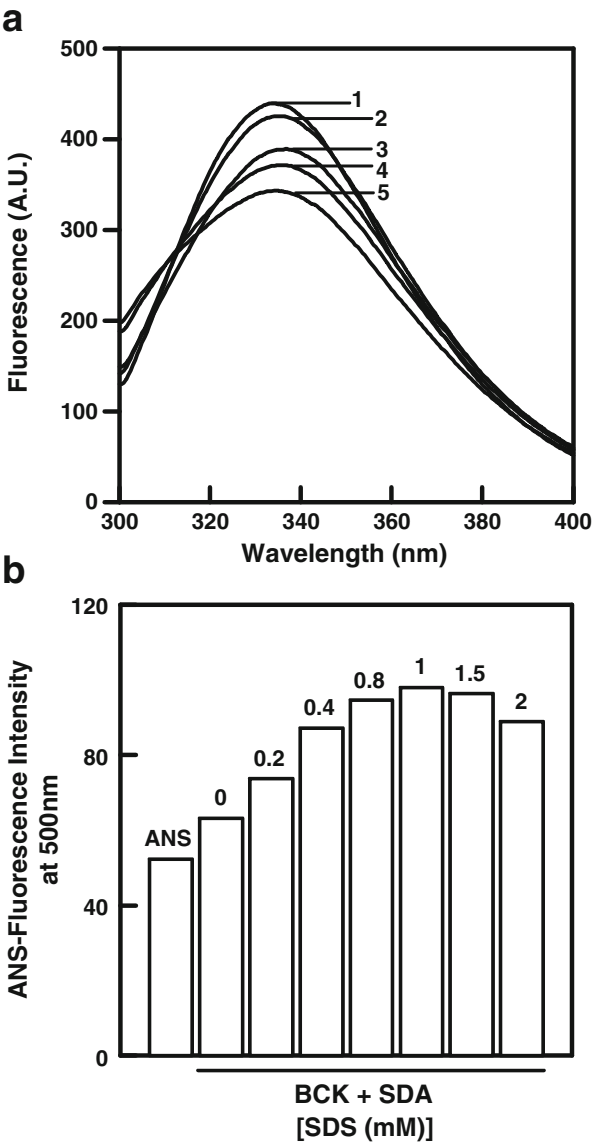

Fig. 5 The intrinsic and ANS-binding fluorescence changes of CK-BB in the presence of different concentrations of SDS. **a** The *labels* (*1* to *5*) show the SDS concentrations as 0, 0.4, 0.8, 1.5, and 2.0 mM, respectively. CK-BB was incubated with SDS for 2 h before measurement. **B** ANS-binding fluorescence changes in the presence of various concentrations of SDS. ANS (40 μM) was incubated for 30 min prior to measurement. The *labels* show the corresponding SDS concentrations

confirmed by the computational docking results. This was also confirmed with the results of changing creatine substrate concentration where the noncompetitive inhibition-binding manner was observed: SDS was directly bound with enzyme molecules instead of being bound to an E–S complex. During the denaturation of a number of enzymes, complete inactivation occurred before there was any noticeable overall conformational change of the enzyme molecule by low concentrations of different denaturants; hence, it was suggested that Tsou's theory [21, 22] applies in that enzyme active sites were formed by relatively weak molecular interactions and were more flexible than the intact enzymes. Our present experiments also supported the view that

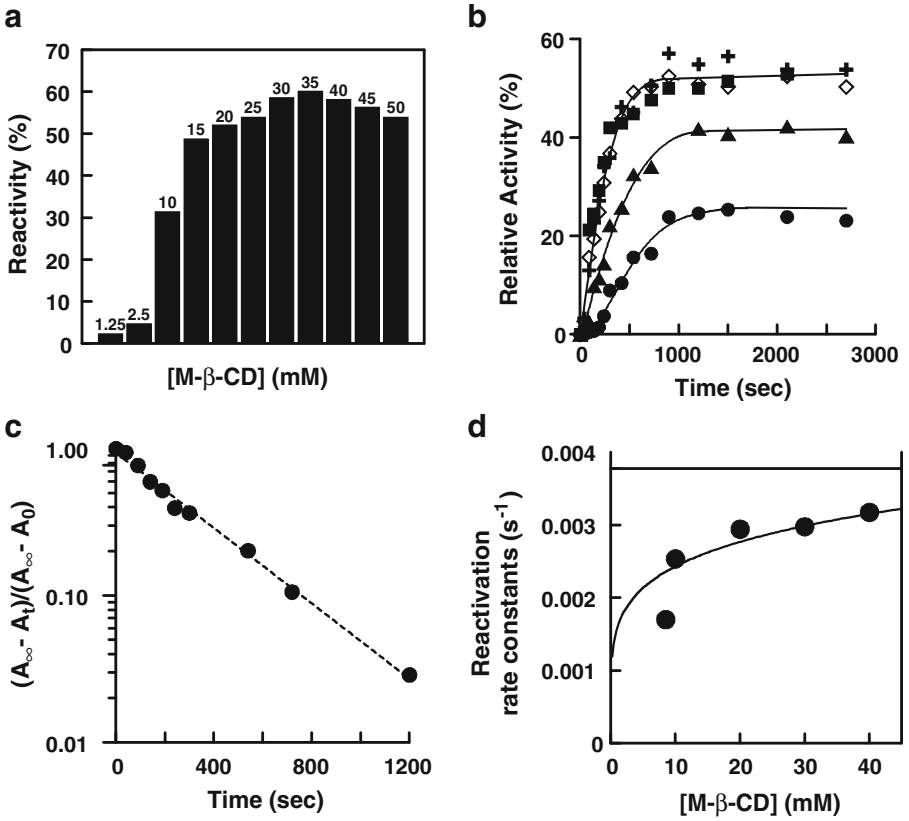

Fig. 6 Reactivation of SDS-inactivated CK-BB in the presence of cyclodextrins. **a** The inactive enzyme sample with 6 mM SDS for 2 h was treated with various concentrations of M-β-CD, and then, the reactivity was assayed after 2 h of incubation. The *labels* show the corresponding M-β-CD concentrations. **b** Kinetic time course for reactivation. The applied M-β-CD concentrations were: 8.5 mM (*filled circle*), 10 mM (*filled triangle*), 20 mM (*open diamond*), 30 mM (*plus sign*), and 40 mM (*filled square*), and aliquots were taken at the indicated time intervals. **c** The semilogarithmic plot in the presence of 30 mM M-β-CD (*filled circle*). **d** Plot of reactivation rate constants versus [M-β-CD]

CK-BB denaturation is a highly cooperative process in the presence of SDS solution. Since the sulfate group and the alkyl chain of SDS bind with the protein via interactions with the positively charged amino acid side chains, it is tightly bound to CK-BB, but cyclodextrin can release SDS specifically from the enzyme molecule with a strong specificity. In the dynamic state during denaturation and renaturation, SDS and cyclodextrin (both have covalent-binding manners) act differently: SDS binding induced a biphasic kinetic process while cyclodextrin-mediated SDS stripping and reactivation was a monophasic process.

Calorimetric Measurements of SDS Ligand Binding to CK-BB

Calorimetric measurement was applied for conducting detailed ligand-binding studies between SDS and CK-BB (Fig. 7). To probe the proper conditions for detection, we

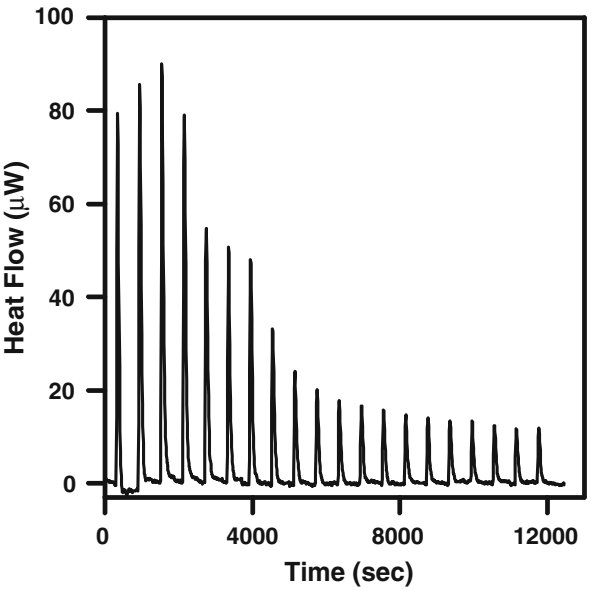

Fig. 7 Isothermal microcalorimetric profile of the titration. A raw calorimetric trace of CK-BB (10 μM) titrated with SDS (200 mM) at 25 °C. For the control, the trace of SDS injected into the buffer, without an enzyme sample, confirmed that it is not changed from the baseline level

adjusted and verified the titration conditions, for example, the SDS and CK-BB concentrations. The thermodynamic parameters are listed in Table 3. Compared to the structural change, that is calorimetric measurement with titration of SDS, ligand binding occurred at a similar order of magnitude at the following molar ratios between SDS and CK-BB. These results indicated the consistency between the structural changes and the isothermal calorimetry.

We conducted the SDS docking simulation on the basis of the computational prediction and revealed that SDS can directly bind to the active site with high docking scores. As CK-BB has a flexible active site, the SDS binding subsequently triggered structural changes and inactivation of CK-BB. From the aspect of physiological function, the results suggest that the metabolic CK-BB function is directly affected by SDS, and therefore, it acts as an environmentally hazardous factor when accumulated in the human body.

Table 3 The thermodynamic parameters for CK-BB in the presence of SDS.

Parameters	Thermodynamic parameters
K	$3.0\times10^{1}\pm5.8$ mol^{-1}
ΔH	−13±7.0 MJ/mol
ΔG	8.39 kJ/mol
ΔS	−42.754 kJ/(K mol)

Data are presented as means ± SD (n=2)

K equilibrium constant, ΔH changes of enthalpy, ΔG Gibbs free energy, ΔS entropy

Acknowledgments This study was supported by a grant from the National Basic Research Program of China (No. 2006CB504100). Dr. Yong-Doo Park was supported by fund from the Science and Technology Planning Project of Jiaxing (No. 2008AZ1024), Zhejiang. Dr. Jong Bhak was supported by a grant from the KRIBB Research Initiative Program of Korea. We thank Maryana Bhak for editing the manuscript.

References

1. McLeish, M. J., & Kenyon, G. L. (2005). *Critical Reviews in Biochemistry and Molecular Biology*, *40*, 1–20. doi:10.1080/10409230590918577.
2. Schlattner, U., Tokarska-Schlattner, M., & Wallimann, T. (2006). *Biochimica et Biophysica Acta*, *1762*, 164–180.
3. Grossman, S. H., & Sellers, D. S. (1998). *Biochimica et Biophysica Acta*, *1387*, 447–453.
4. Abendschein, D. R. (1990). *Clinical Biochemistry*, *23*, 399–407. doi:10.1016/0009-9120(90)90136-I.
5. Aksenov, M., Aksenova, M., Butterfield, D. A., & Markesbery, W. R. (2000). *Journal of Neurochemistry*, *74*, 2520–2527. doi:10.1046/j.1471-4159.2000.0742520.x.
6. David, S., Shoemaker, M., & Haley, B. E. (1998). *Brain Research. Molecular Brain Research*, *54*, 276–287. doi:10.1016/S0169-328X(97)00343-4.
7. Ozawa, E., Hagiwara, Y., & Yoshida, M. (1999). *Molecular and Cellular Biochemistry*, *190*, 143–151. doi:10.1023/A:1006974613418.
8. Schlattner, U., Mockli, N., Speer, O., Werner, S., & Wallimann, T. (2002). *The Journal of Investigative Dermatology*, *118*, 416–423. doi:10.1046/j.0022-202x.2001.01697.x.
9. Takubo, H., Shimoda-Matsubayashi, S., & Mizuno, Y. (2003). *Parkinsonism & Related Disorders*, *9*, S43–S46. doi:10.1016/S1353-8020(02)00121-9.
10. Chen, L. H., White, C. B., Babbitt, P. C., McLeish, M. J., & Kenyon, G. L. (2000). *Journal of Protein Chemistry*, *19*, 59–66. doi:10.1023/A:1007047026691.
11. Mourad-Terzian, T., Steghens, J. P., Min, K. L., Collombel, C., & Bozon, D. (2000). *FEBS Letters*, *475*, 22–26. doi:10.1016/S0014-5793(00)01614-8.
12. John, B., & Sali, A. (2003). *Nucleic Acids Research*, *31*, 3982–3992. doi:10.1093/nar/gkg460.
13. Rodriguez, R., Chinea, G., Lopez, N., Pons, T., & Vriend, G. (1998). *Bioinformatics (Oxford, England)*, *14*, 523–528. doi:10.1093/bioinformatics/14.6.523.
14. Jung, J., & Lee, B. (2000). *Protein Engineering*, *13*, 535–543. doi:10.1093/protein/13.8.535.
15. Huey, R., Morris, G. M., Olson, A. J., & Goodsell, D. S. (2007). *Journal of Computational Chemistry*, *28*, 1145–1152. doi:10.1002/jcc.20634.
16. Moustakas, D. T., Lang, P. T., Pegg, S., Pettersen, E., Kuntz, I. D., Brooijmans, N., et al. (2006). *Journal of Computer-Aided Molecular Design*, *20*, 601–619. doi:10.1007/s10822-006-9060-4.
17. Xie, X. Q., & Chen, J. Z. (2008). *Journal of Chemical Information and Modeling*, *48*, 465–475. doi:10.1021/ci700193u.
18. Han, H. Y., Zou, H. C., Jeon, J. Y., Wang, Y. J., Xu, W. A., Yang, J. M., et al. (2007). *Biochimica et Biophysica Acta*, *1774*, 822–827.
19. Tams, J. W., & Welinder, K. G. (1996). *Biochemistry*, *35*, 7573–7579. doi:10.1021/bi953067l.
20. Rozema, D., & Gellman, S. H. (1996). *The Journal of Biological Chemistry*, *271*, 3478–3487. doi:10.1074/jbc.271.7.3478.
21. Tsou, C. L. (1993). *Science*, *262*, 380–381. doi:10.1126/science.8211158.
22. Tsou, C. L. (1998). *Annals of the New York Academy of Sciences*, *864*, 1–8. doi:10.1111/j.1749-6632.1998.tb10282.x.